

Electron-phonon coupling and its evidence in the photoemission spectra of lead

F. Reinert, B. Eltner, G. Nicolay, D. Ehm, S. Schmidt, and S. Hüfner

Universität des Saarlandes, Fachrichtung 7.2 | Experimentalphysik, D-66041 Saarbrücken, Germany

(Dated: March 22, 2024)

We present a detailed study on the influence of strong electron-phonon coupling to the photoemission spectra of lead. Representing the strong-coupling regime of superconductivity, the spectra of lead show characteristic features that demonstrate the correspondence of physical properties in the normal and the superconducting state, as predicted by the Eliashberg theory. These features appear on an energy scale of a few meV and are accessible for photoemission only by using modern spectrometers with high resolution in energy and angle.

PACS numbers: 71.30.+h, 74.25.Jb, 74.70.Ad, 79.60.-i

A striking evidence of electron-phonon interaction in solids is the existence of superconductivity. Bardeen, Cooper, and Schrieffer showed [1] that even a weak electron-phonon coupling is able to condense two electrons to a so-called Cooper-pair, which is the basic prerequisite of the superconducting ground state and the key feature of the BCS model. The BCS theory describes successfully the superconducting properties of many solids, e.g. Al, V, or V_3Si , where the electron-phonon coupling is sufficiently weak. Other conventional superconductors, e.g. Pb, Hg, or Nb_3Ge , show significant quantitative and qualitative deviations from the predictions of the BCS model [2]. These systems are usually classified as strong-coupling superconductors.

The theoretical approach for the explanation of strong-coupling superconductors is based on the Eliashberg equations, with the coupling function 2F as the central property [3]. This so-called Eliashberg function can be calculated e.g. by first principle methods from the electronic wave functions, the phonon density of states, and the electron-phonon coupling between two Bloch states. However, 2F is a much more universal quantity and determines also the influence of the electron-phonon interaction on the normal state properties, e.g. the electrical resistivity, the electronic heat capacity, and λ as a spectroscopic feature λ the electron-phonon contribution ϵ_{el-ph} to the intrinsic quasi-particle linewidth, which can be determined e.g. by photoemission spectroscopy. In the Green's function method, the influence of electron-phonon interaction is expressed as a contribution to the complex self energy of the conduction electrons ϵ_{el-ph} , which can be calculated from the Eliashberg function 2F [4]. The real part describes the induced band renormalization, where the imaginary part gives the quasi-particle linewidth, equivalent to the reciprocal hole lifetime τ . In particular, at very small energies (i.e. close to the Fermi level), the real part of ϵ_{el-ph} is linear in energy, and $\lambda = \lim_{\omega \rightarrow 0} \frac{1}{\omega} \text{Re}[\epsilon_{el-ph}(\omega)] = \lambda$ at $\omega = 0$ is usually called the mass enhancement factor. In addition, it defines the slope of the temperature dependence of the quasi-particle linewidth $\epsilon_{el-ph} = 2m_{el-ph}^2 k_B T$ for temperatures above the Debye temperature Θ_D .

Photoemission spectroscopy (PES) is a versatile experimental method to study the electronic structure of solids and has been applied to many high- T_c materials [5, 6] and conventional superconductors [7, 8, 9, 10, 11]. Electron-phonon coupling in metallic systems has been studied in detail by PES on low-dimensional electronic states at surfaces, e.g. Shockley-states [12, 13, 14, 15, 16, 17, 18] or quantum-well states [19, 20]. PES investigations on electron-phonon effects in three-dimensional solids, however, are rare. One particularly interesting three-dimensional model system is Pb, which among the conventional superconductors has quite unconventional physical properties.

In the case of Pb the two most relevant energy scales on which the electron-phonon features appear in the spectra, the Debye energy $\hbar\omega_D = k_B \Theta_D$ and the gap width Δ_0 at $T = 0$, define prerequisites that can be met by PES experiments today ($\hbar\omega_D = 7.6$ meV, $\Delta_0 = 1.4$ meV). The instrumental resolution must be at least of the same order of magnitude to give usable spectral information on these features, i.e. $\Delta E \approx 3$ meV. Furthermore, if one wants to measure the band renormalization on single-crystalline samples, the angular resolution must be sufficient to resolve the band dispersion of states close to the Fermi level. Since a few years, photoelectron spectrometers fulfill these requirements and PES has become a unique method yielding access to electron-phonon features in both the density of states and the k -resolved electronic band structure.

The photoemission data presented here have been measured using He I radiation from a monochromatized helium discharge lamp ($\hbar\omega = 21.22$ eV) with an energy resolution of ≈ 3 meV. The angular resolution was typically 0.3° and the sample temperature could be varied from room temperature down to about 4.5 K (see Ref. [9, 21] for details of the experimental setup). The samples were polycrystalline and single-crystalline pellets (Surface Preparation Laboratory, Netherlands), thermally connected to the sample holder by soldered indium. Clean single-crystalline surfaces were prepared in situ by careful Ar sputtering and subsequent annealing at ≈ 150 C.

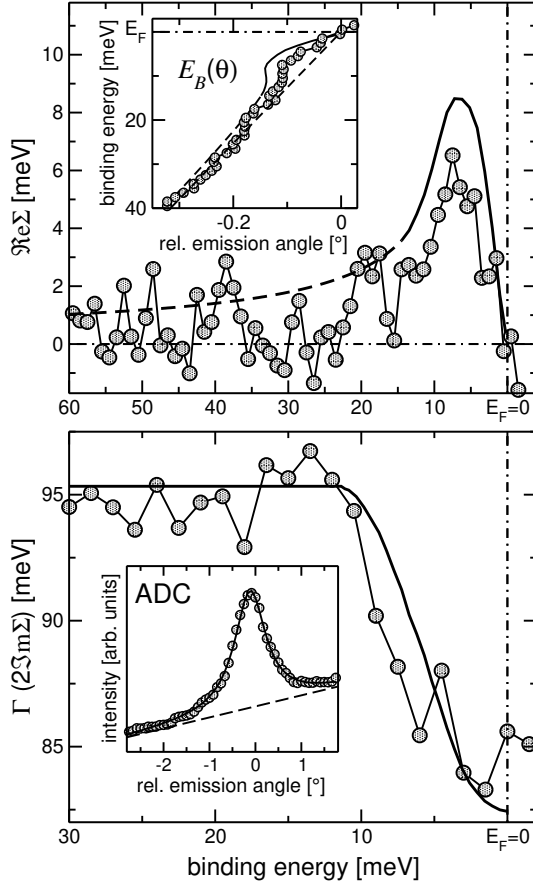


FIG. 1: Real and imaginary part of the electron-phonon self energy, experimental data (circles) and calculated from Ref. [4] (full lines). Upper inset: measured band dispersion close to E_F in the normal phase ($T = 8$ K); the dashed line gives the result of a linear fit to the data points at higher energies ($E_B > 20$ meV). The experimental data points have been determined from the maximum position of a Lorentzian fit to the angular distribution curves (ADC, see lower inset with ADC at $E_B = 10.5$ meV).

On such a surface, one is able to investigate the electronic band structure of states close to the Fermi level by angular resolved PES (ARUPS). The inset in the upper panel of Fig. 1 gives a volume band dispersion E_k close to the Fermi level on a Pb(110) surface in the normal state ($T = 8$ K). With He I, this band, forming the locally tubular Fermi surface of Pb, can be reached slightly off the high-symmetry direction \overline{K} [23], or, more precisely, at $k_{k,x} = 0.82\text{\AA}^{-1}$ along \overline{K} and $k_{k,y} = 0.11\text{\AA}^{-1}$ parallel to \overline{X} . The data points (circles) were determined from the position of the peak maxima in the angular distribution curves (ADC) at the energies close to the Fermi level E_F (see lower inset). At higher energies, i.e. significantly higher than the Debye energy $\hbar\omega_D = 7.6$ meV, the dispersion can be approximated quite well by a linear function of the momentum k , representing the dispersion

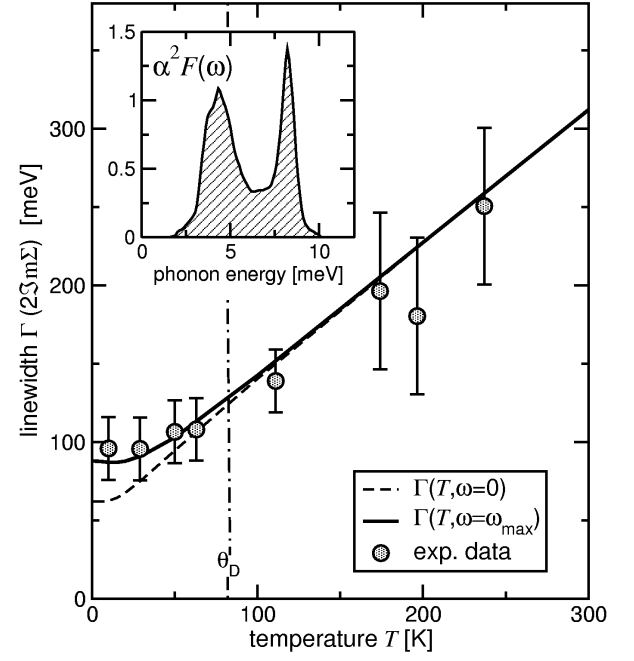


FIG. 2: Temperature dependence of the linewidth for energies $\hbar\omega$ & $\hbar\omega_D$ (circles). The dashed and the solid line represent the calculated electron-phonon contribution at $E_F = 0$ and $E = \hbar\omega_{\max} = 12$ meV, shifted vertically to match the experimental data. The inset shows $\alpha^2 F(\omega)$ as used for the calculation (from Ref. [22]).

ϵ_k with no renormalization. However, below $E = 12$ meV the band shows the wellknown correction due to electron-phonon interaction, which is defined by the real part of the self energy $\langle \epsilon(E_k) \rangle = E_k - \text{Re}\Sigma_k$. The upper panel shows the experimental result ($T = 8$ K) for the deviation from the linear dispersion compared to the calculated $\langle \epsilon \rangle$ from Ref. 4 at $T = 11$ K. The comparison shows a good qualitative agreement, in particular the position of the maximum at 7 meV and the slope at E_F (given by the coupling constant $\lambda = 1.55$) are the same for experiment and theory, within the experimental uncertainties. The difference in maximum height can be explained by the finite experimental resolution. Up to now, such a renormalized quasi-particle dispersion has been observed only for low-dimensional systems, e.g. the Shockley-state on Mo(110) [15] or high- T_c superconductors [5, 6].

By an analysis of the ADC linewidth as a function of the binding energy one can extract the energy dependence of the imaginary part $\text{Im}\Sigma$ of the self energy (see e.g. Refs. 15, 18). The lower panel of Fig. 1 shows the experimental energy dependence in comparison to $\text{Im}\Sigma(E_k)$ from Ref. 4. Since Pb is a three-dimensional system, the contribution of the normal state to the total linewidth can not be neglected [24]. This additional contribution is not related to electron-phonon interaction and therefore does not show an energy or temperature

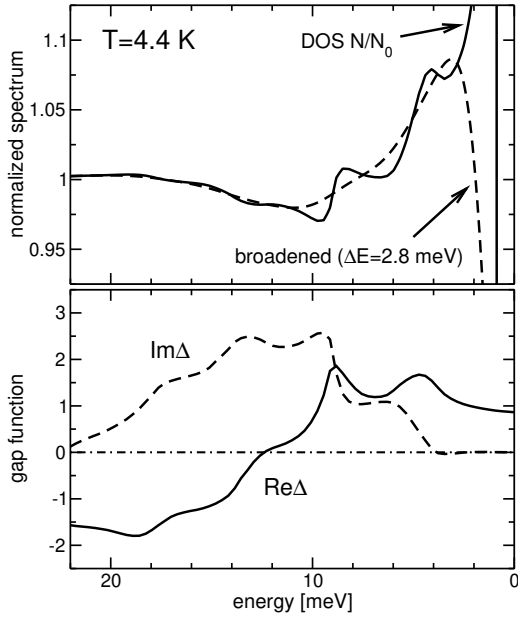


FIG. 3: Lower panel: real and imaginary part of the gap function, interpolated at $T = 4.4$ K from the calculated gap functions at $T = 0$ and $0.98T_c$ given in Ref. [25]. Upper panel: resulting spectrum, raw normalized density of states N/N_0 (solid line) and broadened by a convolution with a Gaussian (FWHM $\Gamma = 2.8$ meV) to simulate the resolution function.

dependence in the investigated range. Thus, it is reasonable to simply shift the theoretical result by 82 meV to match the photoemission data. Apart from this offset and experimental limitations, the agreement between experimental result and theory is good: below the maximum phonon energy ~ 10 meV (see inset of Fig. 2) there is a continuous increase of the linewidth up to a net change of 13 meV. As known from the Debye model, above ~ 10 meV the electron-phonon contribution to the linewidth remains constant.

The photoemission linewidth is also characteristically dependent on the temperature. Fig. 2 shows the experimental linewidth from ADCs for \uparrow and \downarrow (circles); the dashed and the solid line give the theoretical results at E_F and $E_B = \sim 10$ meV, respectively. Obviously, the calculated temperature dependence describes the experiment quite well. For the whole investigated temperature range, the theoretical curve lies within the error bars of the experimental values and, in particular, for high temperatures the experimental linewidth follows the predicted linear behavior given by $\gamma_{\text{el-ph}} = 2 k_B T$, again with $\gamma = 1.55$. This result confirms that the contribution of the normal state to the total photoemission linewidth does not considerably depend on the temperature.

Obviously, there is clear evidence for the strong electron-phonon interaction in the photoemission spectra of Pb in the normal state. In addition, there are characteristic spectral features in the superconducting state

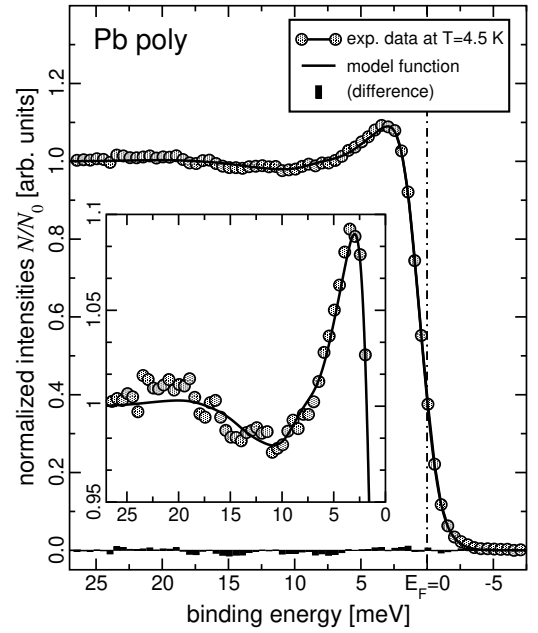


FIG. 4: Comparison of the modelled function from Fig. 3 (solid line) with the experimental data (circles). The black bars at the x-axis indicate the difference between experiment and theory. The inset shows a blow-up of the peak and dip structure.

of Pb: a peak-and-dip structure, that has been experimentally observed first by tunneling techniques [26] and reproduced recently in photoemission data [8]. Theoretically, the density of states of a strongly coupled superconductor can be fully described by an energy and temperature dependent, complex gap function $(E; T)$ given by the Eliashberg theory [27, 28]. The imaginary part of $(E; T)$ is the consequence of the damping of the quasi-particle excitations caused by the electron-phonon interaction. With this gap function, the spectral density of states of a strongly coupled superconductor is described by $N(E; T) = N_0 \cdot \frac{\gamma}{E^2 + \gamma^2}$, giving as a special case the dip-less BCS density of states when chosen real and constant in E .

A theoretical gap function for Pb at finite temperatures can be found in Ref. 25, which gives the energy dependence for $(E; T)$ explicitly for two temperatures $T_1 = 0$ and $T_2 = 0.98T_c$. To obtain the gap function at the temperature of the present experiment ($T = 4.4$ K), we simply interpolated between these two pairs of curves $(E; T) = (1 - (T/T_2)) (E; T_1) + (T/T_2) (E; T_2)$, considering the temperature dependence of the BCS gap [29].

We model the photoemission spectrum by convoluting the result with a Gaussian to describe the broadening from the finite experimental resolution. The interpolated gap function and the resulting spectrum for $T = 4.4$ K are displayed in Fig. 3.

Fig. 4 shows a comparison of the model function with

the experimental data at $T = 4.4$ K, normalized to unity at $E = 27$ meV where the spectrum becomes flat; the inset shows a blow-up of the range of the dip. The solid line represents the model function from Fig. 3, the bars at the x-axis represent the difference to the normalized experimental spectrum. The agreement between experiment and model is striking. Without using any free parameter, all important features – the position of the gap edge, the intensity ratio between peak and dip, and the spectral shape in the displayed energy range – are perfectly described by the model function.

The most important feature of the spectrum in Fig. 4 is the drop of the intensity around 11 meV below unity, which is also lower than the BCS intensity and the normal state DOS in this energy range. Choosing a simple Einstein-like model phonon at energy $\sim E_D$, it was demonstrated [27] that the dip in the DOS appears approximately at a binding energy slightly beyond $\sim E_D + \Delta_0$ corresponding to the maximum position in Δ . This is in accordance with our observation where the dip appears at an energy slightly higher than $\sim E_D + \Delta_0 = 9$ meV. In the BCS model, the superconducting gap width Δ_0 at $T = 0$ is related to the transition temperature T_c by the dimensionless parameter $2\Delta_0/k_B T_c = 3.50$. This parameter amounts to 4.497 for Pb ($T_c = 7.19$ K), much larger than the BCS value; Al ($T_c = 1.18$ K) as the prototype BCS material has 3.535 [2]. This means, the gap width of Pb is larger than for a BCS like superconductor with the same T_c . As a consequence, the characteristic weak photoemission structure from the thermally occupied singularity above E_F , which can be observed e.g. at $T \approx 0.6T_c$ for V_3Si [9], is not resolvable because the Fermi Dirac distribution suppresses the spectral intensity at energies farther away from the Fermi level.

In conclusion, the high-resolution photoemission data presented in this paper clearly demonstrate the influence of the strong electron-phonon coupling on the electronic structure of lead in both the normal and superconducting state. The experimental superconducting density of states, the renormalized band dispersion, the energy and the temperature dependence of the quasiparticle linewidth are in very good agreement with theoretical calculations based on the Eliashberg theory and represent consistently – and even quantitatively – the electron-phonon corrections in spectroscopic data. We hope that these results may also help to reveal the driving mechanisms behind the unconventional superconductors, like high- T_c systems, superconducting heavy-fermion compounds and even superconducting organic materials.

This work was supported by the Deutsche Forschungsgemeinschaft (grant nos. Hu 149-19-1 and SFB 277).

- [1] J. Bardeen, L. N. Cooper, and J. R. Schrieffer, Phys. Rev. 108, 1175 (1957).
- [2] J. P. Carbotte, Rev. Mod. Phys. 62 (4), 1027 (1990).
- [3] G. M. Eliashberg, Sov. Phys. JETP 11 (3), 696 (1960).
- [4] G. Grimvall, Phys. kond. Mat. 9, 283 (1969).
- [5] A. Damascelli, Z. Hussain, and Z.-H. Shen, Rev. Mod. Phys. 75, 473 (2003).
- [6] J. C. Campuzano, M. R. Norman, and M. Randeria, cond-mat/0209476, (2002).
- [7] M. G. Rioni, D. M. Alterre, B. Dardel, et al., Phys. Rev. B 43 (1), 1216 (1991).
- [8] A. Chainani, T. Yokoya, T. Kiss, and S. Shin, Phys. Rev. Lett. 85 (9), 1966 (2000).
- [9] F. Reinert, G. Nicolay, B. Eltner, et al., Phys. Rev. Lett. 85 (18), 3930 (2000).
- [10] S. Tsuda, T. Yokoya, T. Kiss, Y. Takano, et al., Phys. Rev. Lett. 87 (17), 177006 (2001).
- [11] T. Yokoya, T. Kiss, A. Chainani, S. Shin, M. Nohara, and H. Takagi, Science 294, 2518 (2001).
- [12] R. Paniago, R. Matzdorf, G. Meister, and A. Gokhann, Surf. Sci. 336, 113 (1995).
- [13] B. A. McDougall, T. Balasubramanian, and E. Jensen, Phys. Rev. B 51 (19), 13891 (1995).
- [14] T. Balasubramanian, E. Jensen, X. L. Wu, and S. L. Hulbert, Phys. Rev. B 57 (12), R6866 (1998).
- [15] T. Valla, A. V. Fedorov, P. D. Johnson, and S. L. Hubert, Phys. Rev. Lett. 83 (10), 2085 (1999).
- [16] S. LaShell, E. Jensen, and T. Balasubramanian, Phys. Rev. B 61 (3), 2371 (2000).
- [17] A. Eiguren, B. Hellwig, F. Reinert, et al., Phys. Rev. Lett. 88 (6), 066805 (2002).
- [18] M. Hengsberger, R. Fresard, D. Purdie, P. Segovia, and Y. Baer, Phys. Rev. B 60 (15), 10796 (1999).
- [19] J. J. Paggel, T. Müller, and T.-C. Chiang, Phys. Rev. Lett. 83 (7), 1415 (1999).
- [20] K. Takahashi, A. Tanaka, M. Hatano, et al., Surf. Sci. 433/435, 873 (1999).
- [21] F. Reinert, G. Nicolay, S. Schmidt, D. Ehm, and S. Hüfner, Phys. Rev. B 63, 115415 (2001).
- [22] W. L. McDillan and J. M. Rowell, Phys. Rev. Lett. 14 (4), 108 (1965).
- [23] K. Hom, B. Reihl, A. Zartner, et al., D. E. Eastman, K. Hermann, and J. Noke, Phys. Rev. B 30 (4), 1711 (1984).
- [24] N. V. Smith, P. Thiry, and Y. Petrov, Phys. Rev. B 47 (23), 15476 (1993).
- [25] D. J. Scalapino, Y. Wada, and J. C. Swihart, Phys. Rev. Lett. 14 (4), 102 (1965).
- [26] I. Giaever, H. R. Hart, Jr., and K. M. Egerle, Phys. Rev. 126 (3), 941 (1962).
- [27] D. J. Scalapino, J. R. Schrieffer, and J. W. Wilkins, Phys. Rev. 148 (1), 263 (1966).
- [28] J. R. Schrieffer, D. J. Scalapino, and J. W. Wilkins, Phys. Rev. Lett. 10 (8), 336 (1963).
- [29] The weighting factor $\Gamma(T)$ was determined by the ratio of the respective BCS gaps at T and $T = T_2$, resulting in $\Gamma(T) = \Delta_0 / \Delta(T) = \Delta_0 / \Delta(T_2)$.